ECS Transactions, 91 (1) 2737-2747 (2019)
10.1149/09101.2737ecst ©The Electrochemical Society

Reverse Current Treatment of Short Stacks – Experimental Results and System Considerations

M. Hauck[a], S. Herrmann[a], M. Hauser[a], Andreas Geiger[a], F. Fischer[a], J. Weinrich[b], M. Gaderer[b], H. Spliethoff[a]

[a] Technische Universität München, Chair of Energy Systems, 85748 Garching

[b] Technische Universität München, Regenerative Energy Systems, 94315 Straubing/Germany

Anode degradation is one of the main factors that limit the lifetime of solid oxide cells (SOCs), and thus complicate their commercial application. For nickel/yttria-stabilized-zirconia (Ni/YSZ) anodes, one possible counter measure is re-activation through reverse current treatment (RCT). This method has been described for single cells by other researchers. In order to investigate the applicability of RCT in SOC systems, we used this treatment on anode supported short stacks. Two stacks that had been exposed to different degradation phenomena were investigated. The first stack, suffering from partial re-oxidation and a cracked cell, already showed temporary performance improvement after electrolysis operation under mild conditions. The second stack had degraded over a thermal cycle, and different from the first one showed less re-activation. RCT under dry conditions was found to cause severe degradation. Furthermore, we found that, in agreement with literature, YSZ becomes electronically conductive during the RCT, meaning that electrolysis power during RCT is not limited by the amount of available steam. We discuss the issues of this behavior for SOC systems and possible solutions.

Introduction

Solid oxide cells (SOCs) are a promising technology for both efficient and low emission electricity generation, as well as for long-term energy storage through reversible operation (1). During times of high demand, the SOC can produce electrical energy from fossil or renewable fuels including hydrogen, natural gas and bio-fuels. In case of high amounts of fluctuating renewables in the power grid, the SOC works as electrolysis cell to produce hydrogen or carbon monoxide (CO) containing syngas, which can be converted into synthetic natural gas (SNG) or be used for other synthesis processes. The main obstacle for commercialization of SOCs is cost and, connected to that, the limited lifetime. SOCs degrade over time, and state of the art stacks operated as fuel cell need to be replaced after around 40,000 h (2), while continuous electrolysis causes even higher degradation rates and thus shorter lifetimes. Contaminants in the gas supply, thermal stress due to varying load and redox-cycles can cause accelerated degradation.

One way to mitigate these negative effects is through improved materials, that either inhibit a specific degradation mechanism, or increase the tolerance towards certain

contaminants (3–5). These materials are however typically more expensive than conventional Ni/YSZ anodes, and often have a negative effect on performance. Thus, Ni/YSZ fuel electrodes are still used by most manufacturers until today for reasons of cost and performance (6). Therefore, ways to improve performance, or to reduce or revert degradation in such cells and stacks is of high practical interest. The performance of Ni/YSZ anodes can be increased by liquid infiltration with nanoparticles, which increase the amount of triple phase boundaries (TPB) and thus improve kinetics (7). Durability of the introduced particles is a challenge however, and the liquid infiltration cannot be applied during operation. An in-operando method to achieve a similar effect is reverse current treatment (RCT), during which the SOC is subjected to short periods of electrolysis operation under high polarization. During these periods, YSZ is reduced, and subsequently re-oxidized, leading to nanoparticle formation. This again improves the fuel electrode performance by creating additional TPBs (8). Since the possibility to improve cell performance in-operando is highly appealing, several researchers are working on this topic.

Klotz et al. applied RCT on an anode supported single cell manufactured by Forschungszentrum Jülich with an active surface area of 1.0 cm^2 at 700 °C (8). They operated the cell for several hundred hours at OCV before applying four RCTs of 10 s at 2 A/cm^2. 5.5 % humidified hydrogen and air were supplied at a rate of 250 ml/min to the fuel and the air electrode, respectively. Due to the high voltage of up to 2.44 V reduction of YSZ took place. The build-up of a nano-structured layer at the electrolyte-fuel electrode interface, which could be confirmed by SEM, led to a reduction of the fuel electrode polarization resistance of 40%. In a subsequent work, Klotz et al. further investigated the influence of humidity in the hydrogen stream, current density, temperature and RCT duration and frequency. They found that RCT at very dry conditions lead to an increase in area specific resistance (ASR), while at very humid conditions it showed no effect at all. The latter observation was attributed to the lower voltage of less than 2.0 V that was reached at the same current density that was used for the tests with 5% humidified hydrogen (9). It is unclear if RCT would have shown an effect if the current density had been chosen higher. Higher current densities and longer durations lead to a thicker layer of nano particles, with an optimum found for an RCT duration of 40 s. Furthermore they described a characteristic current-voltage behavior for RCTs which feature a shoulder in the voltage at the beginning, and a delayed return to OCV after the current is switched off.

Irvine et al. presented a comprehensive review of the processes occurring at the electrode-electrolyte of SOCs. They described both activation through operation in electrolysis mode under high polarization, as performed by Klotz et al. (9), as well as under high overpotentials during fuel cell operation (10). During the latter, nickel is first oxidized, and then reduced again, leading to new triple phase boundaries similar to the reduction and re-oxidation of YSZ.

Szász et al. further analyzed the reaction mechanism and molecular changes during RCT using scanning transmission microscopy and atom probe tomography (11). They found that during RCT, YSZ is reduced together with nickel, which diffuses towards the electrolyte, forming a nickel-zirkonium-yttrium alloy. This alloy is oxidized upon return to OCV, leaving a nano-scaled, porous layer of (Y,Zr)-oxide. The pores are attributed to oxygen vacancies that form clusters during the RCT (11).

Hauch et al. used RCT on previously degraded cells, and investigated the effect of RCT duration, current density and the effectiveness depending on the preceding degradation mechanism (12). Different from Klotz et al. (8), they combined electrolysis with episodes of fuel cell operation at high current densities, which, according to Irvine et al. (10) should also create additional triple phase boundaries. They found that the fuel electrode kinetics of all cells improved upon RCT, while the ohmic resistance increased. This increase was found to be due to weakening the electrolyte-electrode interface, thereby increasing the contact resistance. This weakening comes with the risk of delamination, which would result in a cell failure. Hauch et al. compared the effect of RCT and constant galvanostatic fuel cell operation and found that the latter only lead to negligible reactivation (12). From this, they concluded that the performance improvement resulted from the short period of electrolysis under high polarization, and not from the episodes of fuel cell operation. While Klotz et al. were able to improve new, non-degraded cells with RCT (8), Hauch et al. reported that they did not observe any improvements in this case (12). This leads to the assumption that the feasibility of RCT depends on the cell characteristics, especially the ones of the fuel electrode – electrolyte interface.

To the authors knowledge, research on RCT so far focused on understanding the fundamental mechanisms through simulations and single cell tests. In this work, we investigate the applicability of RCT on degraded SOC short stacks. We present the different effects on stack performance depending on the preceding degradation mechanism, as well as RCT parameters. Furthermore, we briefly discuss difficulties considering the applicability in commercial systems, and how these could be addressed in the system design.

Experimental

Stack Specifications and Test Setup

Two identical stacks, called stack A and stack B, were tested. They were purchased from Ningbo SOFCMAN Energy Solutions and consisted of five anode supported cells each. The stack design is similar as described elsewhere, with gas supply and exhaust through the bottom plate (13). Differing from the standard design, fuel and air are fed to the stack in counter flow configuration in our case. The stack is built in a cell-to-edge design, meaning that the footprint of the cell is identical to the dimensions of the stack. Each cell has a size of 14 x 14 cm, with an active surface of 130,8 cm². Sealing between cell, interconnector, ambience and gas supply channels is placed directly on the cell. SiO_2-CaO-Al_2O_3 is used for sealing. The stacks were delivered sealed, but not activated. The properties of the stacks are summarized in Table I.

The test set up, which already was described elsewhere (14), consists of an electrically heated furnace, in which the stack is placed, with gas supply and exhaust provided by an adapter plate underneath. Differing from the description in (14), for this work we used a pneumatic cylinder with a 30 mm rod made from AISI 314 steel to compress the stack. Between rod and stack, a 40 mm strong plate of high temperature steel and a 1 mm thick layer of Thermiculite 866 was placed to distribute the force evenly over the stack. The seal between stack and adapter plate was accomplished with a

combination of Thermiculite 866LS and a high temperature sealing glue. This combination was used since the rough surface of the stack bottom plates caused leakages with normal Thermiculite 866 or mica seals. For fuel cell operation, a PLI2106 electronic load from Höcherl & Hackl was used for power control and data acquisition, while for electrolysis a SM 500-CP-90 power source from Delta Elektronika was used. Bottled fuel gas was dosed with mass flow controllers, while steam was dosed by a HPLC pump, which pumped water into a heated metal tube, where it evaporated and mixed with the other gas streams. Gas supply, electronic load and power source were controlled with scripts.

TABLE I. Stack properties.

	SOFCMAN Stack
Number of cells	5
Active surface per cell	130,8 cm²
Flow configuration	Counter flow
Cathode	LSCF+GDC/20-25 µm
Cathode Diffusion Barrier	GDC/2-3 µm
Electrolyte	YSZ/10-15 µm
Anode	NiO+YSZ/400 µm
Sealing material	SiO_2-CaO-Al_2O_3
Interconnect material	AISI 430
Mechanical loading	2256 N

Experimental Procedure before RCT

Stack A was heated to 750 °C at a rate of 4 K/min, and then activated for five hours with 2 Nl/min hydrogen and 2 Nl/min air at the fuel and air electrodes, respectively. Activation of stack B was carried out similarly, except that the heating rate was 1 K/min and the final temperature was 700 °C. Both stacks were operated under direct internal reforming conditions at fuel utilization between 25 and 60 %. I-V curves with dry hydrogen were recorded on a regular basis to monitor changes in performance. Both stacks showed similar initial performance. During pauses in between measurements the stacks were flushed with forming gas (5-10% hydrogen, balance nitrogen). Both stacks were operated mostly in fuel cell mode but were tested in electrolysis mode before RCT to assess their performance. During these tests, the stacks were operated potentiostatically at a cell voltage of 1.33 V.

Stack A suffered from a broken cell, and a subsequently reduced performance. The broken cell was confirmed in a post mortem analysis. Stack B was subjected to a thermal cycle since the test rig had to be shut down for necessary repairs of a defective gas pre-heater. After heating up to 700 °C again, the stack showed severe performance loss. It was unclear which mechanism caused the degradation. Possible explanations are that at some point forming gas supply was insufficient so that anode re-oxidation took place, or that the temperature induced stresses lead to contacting issues or cell damage.

RCT

We conducted RCT at different flow rates, steam content in the fuel gas, duration and current densities. The flow rate was varied between 7.7 and 15.4 Ncm³/min/cm², which is

lower than in previous works (8, 12). The maximum flow rates were limited by the available mass flow controllers, but also represent typical flows that can be reached in power generation systems designed and sized for nominal operating conditions. Steam fraction in hydrogen was varied between 0 (dry) and 30 %. Since the work of other researchers suggests that a voltage of above 2 V is necessary for reduction of YSZ, stack A was operated potentiostatically at a cell voltage of 2.4 V during RCT. Stack B was operated both potentiostatically as well as galvanostatically at voltages between 2.1 and 2.4 V. The duration of the treatments was varied between 10 and 40 s.

Performance assessment

We used current-voltage (IV) curves to assess the performance of stack A and B. The curves were recorded with dry hydrogen before and after the RCT to monitor the change in performance. The operating conditions for stack A and B during IV curves are listed in Table II.

TABLE II. Parameters for IV curve measurement.

	Stack A	**Stack B**
Furnace temperature	715 °C	700 °C
Hydrogen flow rate	2.289 Nl/min	3.05 Nl/min
Air flow rate	6.9 Nl/min	6.9 Nl/min
Load ramp	20 A/min	20 A/min

Fuel flow rates for stack B were chosen higher, since we found through exhaust gas volume flow measurement that a part of the fuel gas was lost through leakages between stack and adapter plate.

Results and Discussion

Both stacks showed a relatively low OCV of around 1.14 V/cell in dry hydrogen, which can be attributed to leakages inherent to the stack design. As the stacks are built in a cell-to-edge design, the sealing on the fuel electrode side is applied onto the support layer. We assume that during activation with hydrogen the support layer under the sealing becomes porous and creates pathways for crossover between air and fuel. Air entering the fuel electrode side partially oxidizes the fuel, forming steam and lowering the OCV. Besides the observed low OCV, this assumption is based on the observation that we found nitrogen in the fuel exhaust, and hydrogen in the air exhaust. Since the air flow is roughly twice the hydrogen flow during most measurements, and subsequently the pressure loss on the air side is higher than on the fuel side, we assume that the dilution of fuel with air was the main reason for the low OCV, and that the crossover of fuel to the oxygen electrode had only a minor effect.

Stack A. Figure 1 shows several IV curves recorded over time. The stack showed the highest performance in the beginning (‘Initial’). The unsteady course of the curve is caused by the control parameters of the electronic load. The initial performance strongly degraded after a cell broke, shown by the curve ‘After degradation’ in Figure 1.

After that, stack A was operated in electrolysis mode for several hours at 1.33 V/cell. The IV curve recorded after that showed a significant regeneration, almost back to its

initial performance ('After mild electrolysis'). This regeneration however was only temporary, and after two hours of fuel cell operation the performance dropped to the previous level again (not shown). We assume that in the damaged stack layer, air crossed to the fuel electrode through the crack in the cell, where it re-oxidized adjacent regions of the fuel electrode. During electrolysis, hydrogen was formed directly at the affected electrode-electrolyte interface, reducing and thus re-activating these parts of the cell. Since air could still enter the fuel electrode through the crack, the affected regions were re-oxidized under fuel cell operation in the end.

Following the renewed degradation, several RCTs with different fuel flow rates and durations were conducted at a constant voltage of 2.4 V/cell. Since all of them showed a similar pattern, only one is depicted in Figure 2.

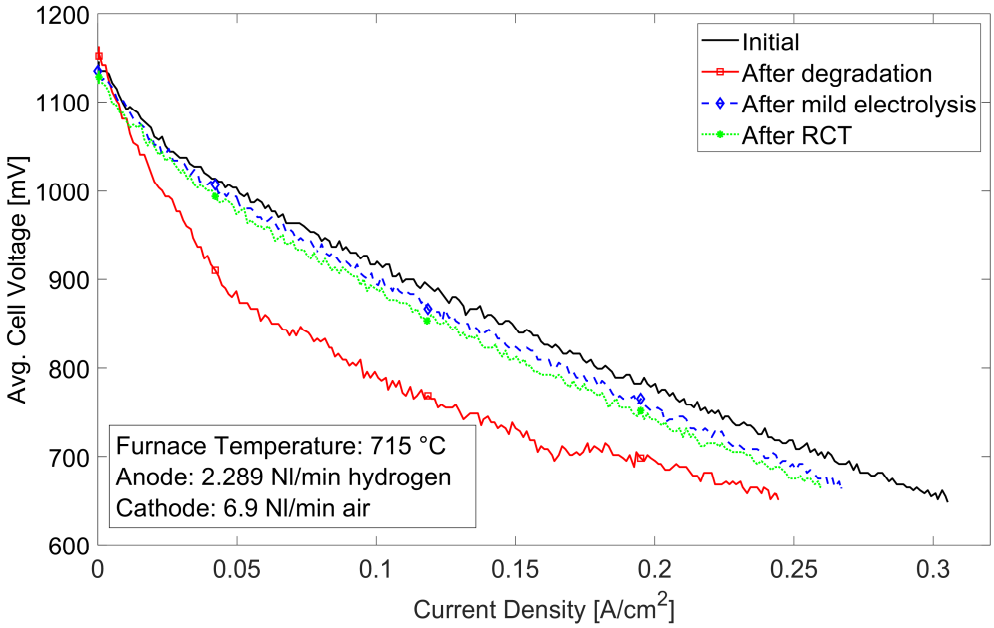

Figure 1: IV curves for stack A.

While the voltage was constant, the current increased over time. This is consistent with the findings of other researchers, who performed RCT under galvanostatic conditions and observed a decline in voltage over time. When the RCT was terminated, the current dropped instantaneously, while the voltage returned to OCV with a slight delay, as reported in literature. The current density shown in Figure 2 was substantially higher than the maximum possible current density from steam reduction. This can be explained by the electronic conductivity of YSZ at higher voltages. This agrees well with the observation that the current during RCT was only slightly affected by the amount of available steam. The effect on stack performance was similar, though smaller, than the one of electrolysis at 1.33 V/cell, depicted in Figure 1 ('After RCT'). Additional RCTs did not further alter stack performance. Possible reasons why no further performance improvement could be achieved are that either no nano-scaled layer was formed, that the formed layer was ineffective, or that unwanted side effects (e.g. increased ohmic resistance) countered the improvement of the fuel electrode (11). All of these reasons might be connected to improper parameters for the RCT.

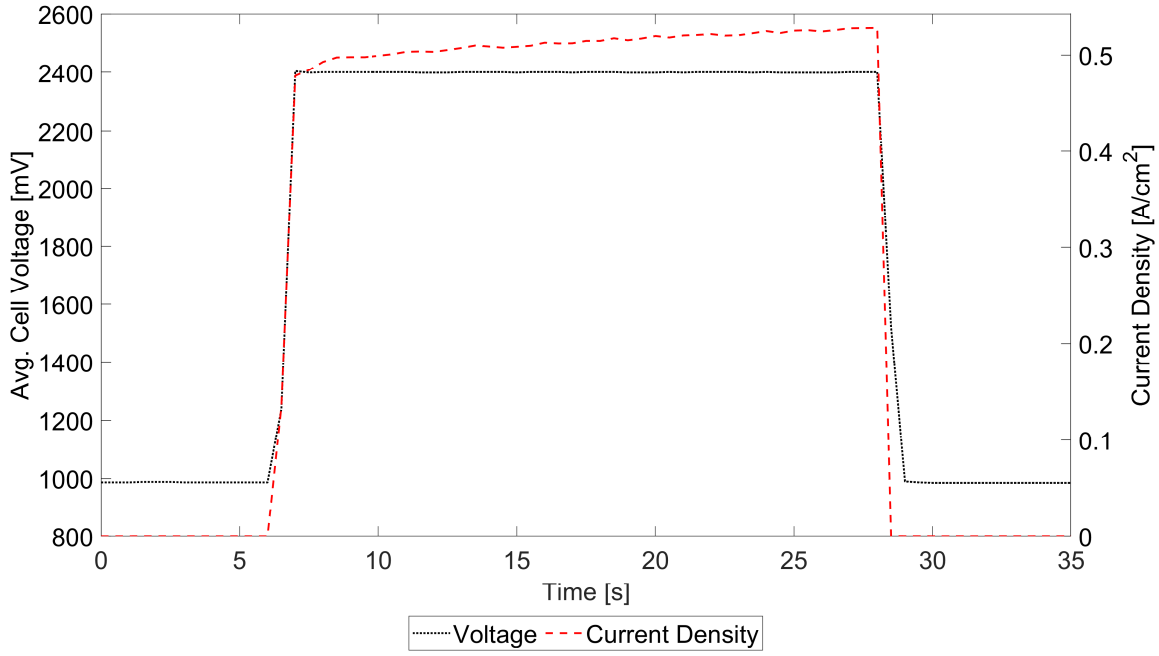

Figure 2: RCT of stack A at 715 °C with 3.5 Nl/min hydrogen, 30 % humidified.

Stack B. The performance of stack B at different times is depicted in Figure 3. The control of the electronic load was adapted to avoid the unsteady behavior visible in Figure 1. Performance degradation from the initial state ('Initial') occurred after a thermal cycle due to unknown reasons. Since the fluctuations in the respective curve ('After degradation') were not caused by the measurement device, they were attributed to the stack itself. One possible explanation could be partial re-oxidation of the stack. The stack was operated in fuel cell mode for several hours without substantial performance changes.

After few minutes of electrolysis operation at 1.33 V/cell however, performance slightly improved ('After mild electrolysis'). Besides that, also the fluctuations vanished. This observation leads us to the assumption that the mechanism behind the degradation was different from stack A. While in case of stack A, performance could be almost completely recovered through electrolysis operation, stack B showed only a minor improvement.

Following electrolysis at 1.33 V/cell, a RCT at 2.1 V/cell with 10 % humidified hydrogen was performed. The voltage source was switched on again after the gas stream had been changed to dry hydrogen already. This unplanned dry RCT is depicted in Figure 4. Different from Figure 2, the current did not increase over time, but decreased. Looking at the initial OCV, this can be explained by remaining steam in the hydrogen, which was still present at the beginning of the RCT. As this steam was reduced, the current declined. Another difference was the larger delay between voltage and current. Especially when the RCT was terminated, it took around five seconds for the voltage to reach OCV again. The dry RCT caused a performance degradation, as shown in Figure 3 ('After dry RCT'). The voltage under load subsequently began to fluctuate strongly (not shown), indicating that

the stack had been severely damaged. These findings agree well with those of Klotz et al., who also found that RCT under dry conditions increased the ASR (9). Attempts to regenerate the stack with further RCTs in 5-30 % humidified hydrogen showed no effect.

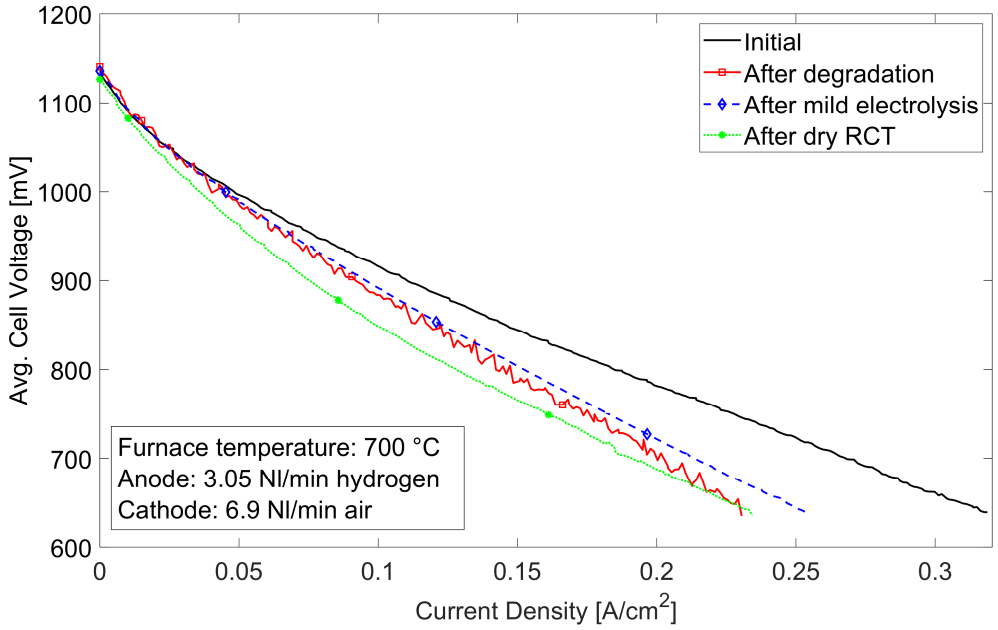

Figure 3: IV curves for stack B.

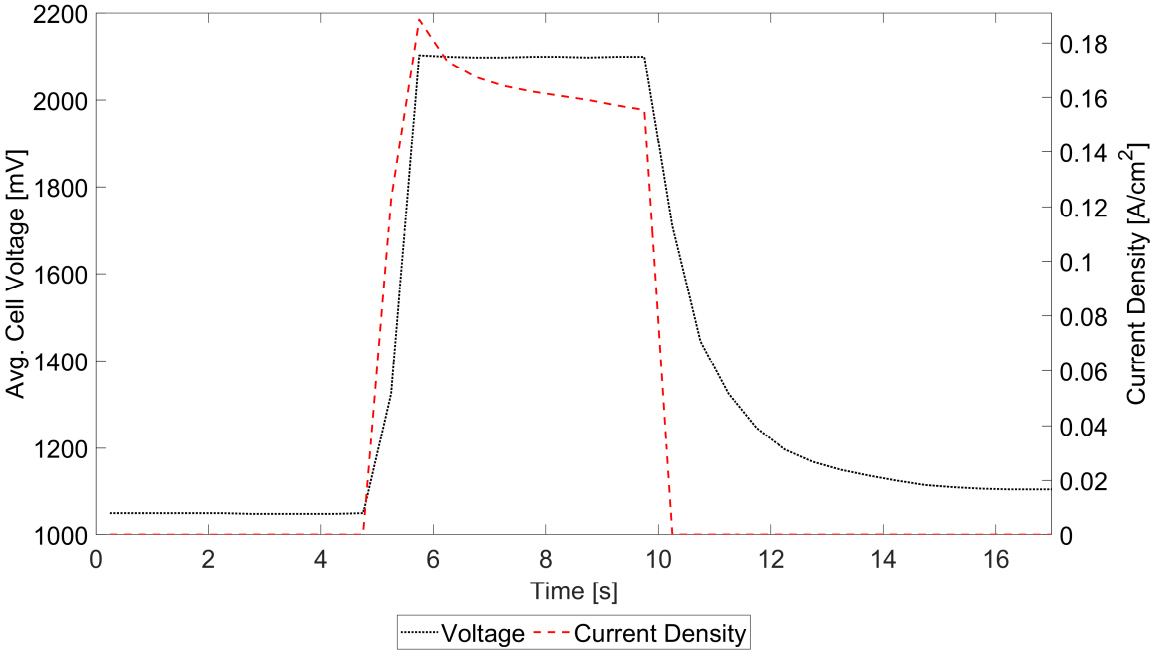

Figure 4: RCT of stack B at 700 °C with 3.05 Nl/min hydrogen, dry.

While in the present work no performance improvement through RCT beyond the one accomplished with normal electrolysis could be reached, we observed the typical current-

voltage behavior reported for single cells also on stack level. The dry RCT performed on stack B showed that the treatment affected the stack, indicating that with a better choice of parameters also a positive effect on stack performance should be feasible. These findings point out that, before applying RCT to stacks, extensive study on single cells of the same design as used in the stack are recommended to identify operating parameters.

System Considerations

The relevance of RCT for commercial application depends on the additional investment costs that are necessary to perform this kind of treatment. Most SOC systems today are designed as non-reversible, power generation only plants. Therefore, they are not equipped with the necessary power electronics to perform electrolysis. Even electrolysers or reversible systems face the issue that the power consumption during RCT is very high. For the investigated stacks we found that the power consumption depended more on the applied voltage, and less on the amount of available steam. At a cell voltage of 2.1 V, it was more than 2.5 times the maximum power output in fuel cell mode, while at 2.4 V it went up to a factor of 6 and higher. Power electronics sized for RCT would therefore increase the investment costs and relativize possible cost savings through prolonged SOC lifetime and performance. We therefore propose a novel system configuration, which is schematically depicted in Figure 5.

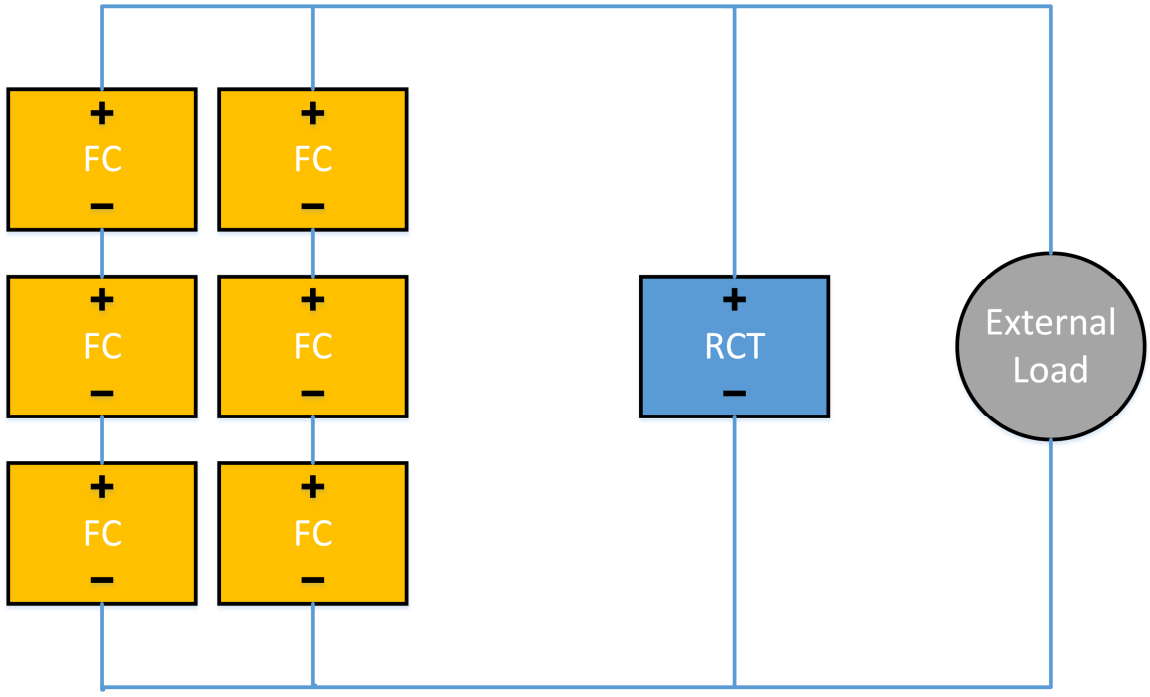

Figure 5: Proposed configuration for RCT. Stacks operating in fuel cell mode (FC) provide power for the stack under RCT (RCT). Excess electrical power can be directed to an external load at constant voltage.

The basic idea is, instead of using external power for RCT, to operate part of the system in fuel cell mode. Prerequisite for this method is that the system consists of several stacks, and that the stacks have separate electrical connections. This way, all stacks can either be connected in series for normal operation, or in the desired

configuration for RCT. Considering that a cell voltage of above 2 V is necessary for YSZ reduction, for each cell that is subjected to RCT, three cells connected in series must run in fuel cell mode at 0.7-0.8 V each. Considering current, the lower the RCT voltage, the less current is drawn by the treated stack, and the more current is provided by the stacks operated in fuel cell mode. We assume that the optimal voltage for RCT depends largely on the cell properties, and so does the power demand. If the treatment is to be performed at around 2.1 V/cell, three stacks connected in series can most probably supply sufficient current. For higher voltages, two three-stacks-in-series-arrangements need to be connected in parallel. The power electronics used during normal fuel cell operation could be hooked in parallel to the treated stack and set to potentiostatic operation mode to control the voltage during RCT. If the system uses off-gas recirculation, the steam produced by the stacks in fuel cell mode can be used to humidify the fuel to the desired level.

The presented concept only requires little changes to conventional system layouts. More high temperature cables are needed, as well as additional power switches to connect stacks in the desired configuration, but these are estimated to cost much less than additional power electronics.

Conclusion

In this work we investigated the applicability of RCT on stacks. We found that degraded stacks can be partially and temporarily regenerated by electrolysis operation under mild conditions, depending on the degradation mechanism. The attempt to apply RCT at voltages between 2.1 and 2.4 V in humidified hydrogen did not lead to any performance improvement beyond the one reached with mild electrolysis, while RCT under dry conditions caused severe and permanent degradation. The observed evolution of voltage and current during RCT however followed the qualitative trends described in literature for treatment of single cells. Therefore, we conclude that the cell structure can be altered with RCT also in stacks, while the treatment parameters have to be chosen carefully with respect to the cell properties. Furthermore, we present a concept for SOC systems that can perform RCT with only little changes to the system layout and investment costs.

In future work, we will investigate single cells with the same properties as the ones used in the stacks with help of EIS. We will then identify advantageous operating parameters for RCT, and then transfer these to stack level.

Acknowledgments

The presented work has been funded by the German Federal Ministry of Education and Research in the frame of the project BioCORE, which is gratefully acknowledged.

References

1. C. H. Wendel, P. Kazempoor and R. J. Braun, *Journal of Power Sources,* **276,** 133–144 (2015).
2. M. Bertoldi, O. F. Bucheli and A. Ravagni, *ECS Trans.,* **78**(1), 117–123 (2017).
3. T. Klemensø, K. Thydén, M. Chen and H.-J. Wang, *Journal of Power Sources,* **195**(21), 7295–7301 (2010).
4. J. Mermelstein, M. Millan and N. Brandon, *Journal of Power Sources,* **195**(6), 1657–1666 (2010).
5. C. M. Finnerty, N. J. Coe, R. H. Cunningham and R. M. Ormerod, *Catalysis Today,* **46**(2-3), 137–145 (1998).
6. J. Hanna, W. Y. Lee, Y. Shi and A. F. Ghoniem, *Progress in Energy and Combustion Science,* **40,** 74–111 (2014).
7. Y. Lu, P. Gasper, U. B. Pal, S. Gopalan and S. N. Basu, *Journal of Power Sources,* **396,** 257–264 (2018).
8. D. Klotz, Butz, A. Leonide, J. Hayd, D. Gerthsen and E. Ivers-Tiffe´, *Journal of The Electrochemical Society,* **158**(6), 587–595 (2011).
9. D. Klotz, J. Szasz, A. Weber and E. Ivers-Tiffee, *ECS Transactions,* **45**(1), 241–249 (2012).
10. J. T. S. Irvine, D. Neagu, M. C. Verbraeken, C. Chatzichristodoulou, C. Graves and M. B. Mogensen, *Nat. Energy,* **1**(1), 15014 (2016).
11. J. Szász, S. Seils, D. Klotz, H. Störmer, M. Heilmaier, D. Gerthsen, H. Yokokawa and E. Ivers-Tiffée, *Chem. Mater.,* **29**(12), 5113–5123 (2017).
12. A. Hauch, M. Marchese, A. Lanzini and C. Graves, *Journal of Power Sources,* **377,** 110–120 (2018).
13. Le Jin, W. Guan, X. Ma, H. Zhai and W. G. Wang, *Journal of Power Sources,* **253,** 305–314 (2014).
14. F. Fischer, M. Hauser, M. Hauck, S. Herrmann, S. Fendt, H. Jeong, C. Lenser, N. H. Menzler and H. Spliethoff, *Energy Sci Eng,* **40,** 270 (2019).